Numerical analysis of the cathodic material influence on the arc plasma jet

D.F. Devia-Narváez[a,*], L.F. Álvarez-Correa[b], S. Ramírez-Ramírez[c], and E. Restrepo-Parra[c]
[a]*Grupo de Ecuaciones Diferenciales y Aplicaciones, Universidad Tecnológica de Pereira.*
[*]*e-mail: dfdevian@utp.edu.co*
[b]*IDEXA, Escuela de Ingeniería Mecánica, Universidad del Valle.*
[c]*PCM Computational Applications, Universidad Nacional de Colombia, Sede Manizales.*

Received 10 October 2018; accepted 12 November 2018

The cathodic arc discharge is a deposition technique widely used to synthesize hard coatings and thin films. The structure of the plasma generated by the electrical discharge and its interaction with neutral particles was studied using numerical simulations. Typical plasma parameters were characterized considering their spatial and temporal dependence, as well as several cathode materials that are commonly used in these systems. For the evolution of the ion density, it was observed the formation of Knudsen layer, and also a dependence of pressure gradients in the global behavior. With respect to the kinetic energy, it was found a deceleration of ions, which is represented by a shock front produced in the plasma−neutrals interaction. On the other hand, the energy releasing was generated due to the heat transference between electrons and ions. The plasma potential follows a behavior, which is similar to that of the ion density, and it is caused by the dynamics of charged particles which is directly affected by the concentration of neutrals and ions. In general, the physical quantities are directly affected by electrical and thermal conductivity of the cathode material. Our results can be applied to understand the plasma phenomena produced in a cathodic arc discharge.

Keywords: Arc discharge; materials processing; cathode material.

PACS: 52.20.-j; 52.25.-b; 52.27.-h.

1. Introduction

Industrial and technological development has increased the materials technology demand, focused on increasing the performance of industrial pieces by improving the behavior of its surface. The cathodic arc deposition is a process successfully used for this purpose, due to its wide area of applications in hard and decorative coatings [1,2]. The discharge process uses a power supply to generate an electric arc between two electrodes of high current and low voltage, which is directed toward a cathodic target. This target is usually the desired material to be deposited, as a coating, onto a surface. As a result of the energy stream produced in the discharge, a small a numerous discrete sites of high current density in the range between 10^{11} and 10^{13} A/m^2 are formed on the target surface. This sites are called cathodic spots [3]. In these spots, the electrical heating causes a thermal evaporation of the material. In a properly deposition system, this vapor can be condensed onto the substrate forming a hard coating. In the discharge dynamics, a large fraction of the ion flux is directed toward the anode; however, another percentage of this flux goes far from the interelectrode region toward an empty zone between the electrodes and the chamber wall. As a consequence, the increasing concentration of ions in this zone could generate an electrostatic potential, which can drag electrons from the discharge region in order to neutralize it, therefore, a plasma is produced. As for the plasma generated in that region, few theoretical and experimental studies have been developed, since the scientific community is focused on understanding the chemical and physical processes taking place in the bulk region between the electrodes (discharge region) [4,5]. Nonetheless, some authors have studied the plasma structure in the surroundings of a cathodic arc discharge.

The first studies of the gas−plasma interaction were carried out by Boxman and Goldsmith [6] using numerical simulations. They studied, in the case of an arc in a low-pressure background gas, the balance between the pressure of a surrounding gas and the momentum flux density formed by cathode-spot plasma jet. Their theoretical model relates R, p, and I, following the relation $R^2p/I =$ constant scaling law. Despite the fact that their model reproduced favorably experimental data, there were several unexplored mechanisms behind these processes. The pioneering authors in this work are Kelly, Minotti, and Márquez. They have developed both experiments and simulations of these phenomena. For instance, in numerical simulation, Kelly *et al.* [7] started from a stationary two-fluid model describing the region surrounding the electrodes of a multi-cathode-spot vacuum arc. An important feature of the model was a prediction of a voltage profile outside the electrodes, causing an acceleration of the ions arisen from the discharge region. Nevertheless, that model did not include the interaction between plasma and neutral gas; thus, a more realistic model was developed by Kelly *et al.* [8]. They presented a stationary fluid model to describe the interaction between metallic plasma ions with neutral particles. Their results confirm the expansion mechanism in which the particles are heated during the transient state of the metallic plasma proposed by Meunier *et al.* [9]. Furthermore, the model predictions about the behavior of plasma density, ion flux attenuation and electron temperature were confirmed using electrostatic probe measurements by Grondona *et al.* [10] and Bilek *et al.* [11]. However, some

corrections of that model were developed by Kelly *et al*. [12], for instance, the inclusion of metallic−ion recombination. A principal conclusion of that study was the description of the ion slowing down by elastic scattering with neutral particles.

Some experimental measurements of plasma-gas interaction in the outer region of a low-pressure cathodic arc were presented by several authors [13-17] confirming the most relevant results from theoretical models described above. Minotti *et al.* [18] presented a more realistic model. They developed a two−dimensional model in a cylindrical geometry, taking into account elastic collisions, charge−exchange reactions, and the generation and recombination of gaseous ions by electron impact. Experimental comparison has not yet been made to this model; however, the profiles obtained along the radius are in concordance with those determined by the models described above.

Despite the fact that theoretical models are approximately in good agreement with experimental data, there are some questions about the influence of non-stationary transition, and time dependence of the ions velocity distribution that are still not solved. Gidalevich *et al.* [19] proposed a hydrodynamic model for the plasma jet interaction with a neutral background gas. They analyzed the isothermal gas motion and gas motion with energy transfer from the ions to the neutrals during the initial non-stationary stage of a vacuum arc plasma jet interaction with neutral gas. They found that the plasma front expands with decreasing velocity and also, the neutral gas is accelerated by the plasma jet up to supersonic velocity. Several models using two-fluid model and hydrodynamic description have been developed, however, a complete study of the phenomena was not clearly obtained. Thereby, in this work, we revisit the issue about interaction between plasmas and neutral background gases in a cathodic arc discharge. We employed a spherically symmetric fluid steady model developed by Kelly *et al.*, [12] to describe the plasma-gas structure generated in a low-pressure arc. In spite of the model considerations employed by Kelly *et al.*, we included the temporal dependence of the ion density in the ion continuity equation, electron temperature in the electron energy balance equation, and ion velocity in the conservation of ion momentum, which allowed us to obtain a temporal dependence of ion density, kinetic ion energy, electron temperature and electric potential. Also, the spatial, and temporal dependence of the plasma behavior was characterized using numerical simulations for different cathode materials that are commonly used in a cathodic arc deposition. The study of the structure and state of the plasma around the cathodic arc discharge represents a relevant step to understand the complete phenomena of mechanisms involved in materials deposition. The generation of an electrostatic potential produced by the plasma, and the interaction between metallic plasma and neutral gas, such as elastic collisions and charge-exchange reaction, have a strong influence on the ion energy, and ion flux distribution. For instance, Changji *et al.* [20] found that the energy of Zr (Zirconium) ions arriving at the substrate decreases significantly with the deposition pressure. This effect explains the fact that the adhesion decreases as the deposition pressure increases. Other example is showed by Zhu *et al*. [21], they found a preferred orientations of MgO (Magnesium oxide) films as a function of pressure. They concluded that the increase of the background O_2 (Oxygen) gas pressure results in a decrease in the kinetic energy of the depositing metallic species. Therefore, the crystalline quality of the film decreases with further increasing gas pressure. Another interesting contribution of these studies is the determination of a base structure to study the atomic processes happening in the discharge, which is a necessary step for the interpretation of spectroscopic measurements in the cathodic arc deposition.

An outline of the paper is presented as follows: Sec. 2 shows the formulation of the model; Sec. 3 describes the numerical simulation; finally, in Sec. 4, we summarize our conclusions of the results.

2. Model Description

We present a set of equations that represent the spatio-temporal evolution of the plasma−arc plasma jet interaction during an arc discharge. The model has been based on a previous model developed by Kelly *et al.* [12], which describes a steady state interaction between metallic plasma and neutral gas. Nevertheless, we included the temporal dependence of the ion density (n_i), electron temperature (T_e), and ion velocity (v_i). This modification, allows us to obtain the time and spatial dependence of some plasma parameters as kinetic energy (E_i), electrostatic potential (ϕ), the electron temperature (T_e), and ion density.

The model is applied to systems where multiple spots that enhance the cathode erosion are produced. In most cases, arcs at low current produce a single cathode spot and, as the current is increased, another cathode spots appear in a proportional way, producing a plasma jet of high velocity that

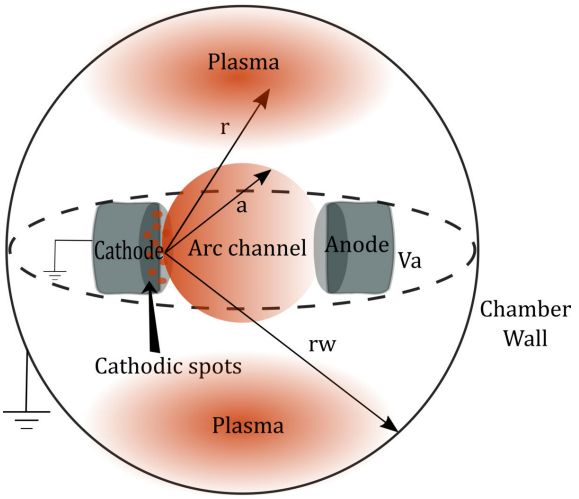

FIGURE 1. Sketch of the discharge chamber constituted by two electrodes (cathode and anode). The plasma surrounding the discharge channel is produced as a result of ion expansion from cathodic spots.

FIGURE 2. Experimental result of the spherical plasma flux from a cathodic arc discharge. The experiment was performed using a titanium cathode with combination of Argon and Nitrogen gases, and using a current of 60 A, voltage of 270 V, and a pressure of 1.7 mbar.

fills the whole interelectrode space [9]. This plasma follows the quasi-neutrality principle due to the small values of Debye Length, $\lambda_D \sim 2 \times 10^{-6}$ cm.

A geometrical scheme of the region, where the plasma is generated, is shown in Fig. 1 and it is represented by a spherical discharge chamber containing two electrodes facing each other, whose walls and cathode are grounded. The spherical symmetry consideration can be a suitable approximation since the plasma flux and energy dissipation are expanding spherically, which is in agreement with our own experimental results, as it is shown in Fig. 2. This experiment was performed using a titanium cathode with combination of Argon (Ar) and Nitrogen (N) gases, and it was used as discharge parameters a direct current of 60 A, voltage of 270 V, and a pressure of 1.7 mbar. This result was corroborated by other authors using a cylindrical anode with cathode placed at the center of symmetry [22]. Besides, the angular dependence (θ, φ) is neglected for simplicity of the model. Moreover, the other variables of Fig. 1 correspond to the radius of the arc discharge (a), the chamber wall radius (r_w), and anode at voltage (V_a).

The model developed by Kelly *et al.* [12] is based on two fluid theory and considers the density, momentum conservation and energy equations for a given plasma species The physics behind the model is briefly described. The Eq. 1 describes the ion continuity and has the form:

$$\frac{\partial n_i}{\partial t} + \frac{1}{r^2}\frac{\partial}{\partial r}\left(r^2 n_i v_i\right) = -\frac{1}{z_r}\sigma_{\text{loss}} n_i v_i N_n, \qquad (1)$$

where v_i is the ion velocity, z_r is an average charge, N_n is a polynomial function obtained from Ref. [12], which represents the spatial evolution of neutral particle density, and $\sigma_{\text{loss}} = 2 \times 10^{-17}$ cm^{-2} is the cross section of the recombination produced by neutral$-$ion losses. The left terms of this equation represent the advection effects of ion density (n_i) and the right hand side corresponds to sink term.

On the other hand, the model contains the momentum conservation for ions, and it is described as:

$$\begin{aligned} m_i \frac{\partial v_i}{\partial t} + m_i v_i \frac{\partial v_i}{\partial r} = &-\frac{1}{n_i}\frac{\partial}{\partial r}\left(n_i T_n\right) \\ &- z_r e \frac{\partial \phi}{\partial r} + R_{ie} \\ &- \frac{1}{2} m_i v_i^2 N_n \left(\frac{2m_n}{m_i + m_n}\right)\sigma_{in}, \end{aligned} \qquad (2)$$

where ϕ is the electrostatic potential, m_i and m_n are the ions and neutral masses, respectively, e is the electron charge, T_n is the temperature of neutral particles, $\sigma_{in} \approx 10^{-19}\,\text{m}^2$ corresponds to the collision cross section for ions [23] and R_{ie} is the collisional moment. Left hand terms correspond to inertial forces in the plasma species, which are balanced by the sum of forces (right terms) acting on the fluid motion. The expansion of plasma is governed by pressure gradients (∇p) contained in the first right terms, and because the energy of particles is small compared with kinetic energy, it is possible to approximate the plasma as a perfect gas. In this way, the pressure can be written as $p = n k_B T_e$. Those pressure gradients are associated with changes in charge particle densities which generate electrostatic potential gradients, represented in the second right hand terms. The third right term of this equation represents the frictional forces arising from the interaction between electrons and ions. Finally, the fourth term is associated to the cross section of elastic collisions between ions and neutral particles.

Moreover, following the same model and physical behavior for the momentum conservation for electrons, it is obtained:

$$\begin{aligned} 0 = &\frac{1}{n_e}\frac{\partial}{\partial r}\left(n_e T_e\right) - e\frac{\partial \phi}{\partial r} - R_{ei} \\ &+ m_e v_e N_n \left(\frac{T_e}{m_e}\right)^{1/2}\sigma_{en}, \end{aligned} \qquad (3)$$

where n_e is the electron density, T_e is the electron temperature, m_e is the electron mass, and $\sigma_{en} \approx 10^{-20}\text{m}^2$ corresponds to the collision cross section for electrons [23]. The left term of this equation is zero because m_e is negligible compared to m_i and m_n. This is consistent because these transport processes occur in a collision-dominated limit. Finally, R_{ie} is constituted by combined ion-electron friction effects. Kelly *et al.* [12] used in their model an expression given by:

$$R_{ie} = -z_r R_{ei} = -\frac{1}{\sigma} e^2 z_r^2 n_i v_i + \beta \frac{\partial T_e}{\partial r}, \qquad (4)$$

where β is the Braginskii's thermoelectric coefficient.

Moreover, we consider the plasma in a quasi$-$neutrality state. Nevertheless, the cathodic emission produces several ion species, giving as a result, differences in kinetic energy and ionization degree. Then, for simplicity, we consider an unique ionic specie with an average energy and charge. Also,

TABLE I. Constants used for different materials and initial conditions for a radius arc $a = 0.5$ cm .

Cathode material	m_i (g)	$\sigma\left(\frac{\text{S}}{\text{cm}}\right)$	$\kappa_e\left(\text{Wm}^{-1}\text{K}^{-1}\right)$	z_r (adim)	$T_e\,(a)$ (eV)	$v_i\,(a)\left(\frac{\text{cm}}{\text{s}}\right)$	$\phi\,(a)$ (V)
Cu	1.05×10^{-22}	1.16×10^{-41}	401	2.06	3.5	1.32×10^{6}	23.4
Ti	7.95×10^{-23}	8.84×10^{-42}	22	2.03	3.2	1.54×10^{6}	21.3
Zr	1.51×10^{-22}	1.67×10^{-41}	23	2.58	3.7	1.54×10^{6}	23.4

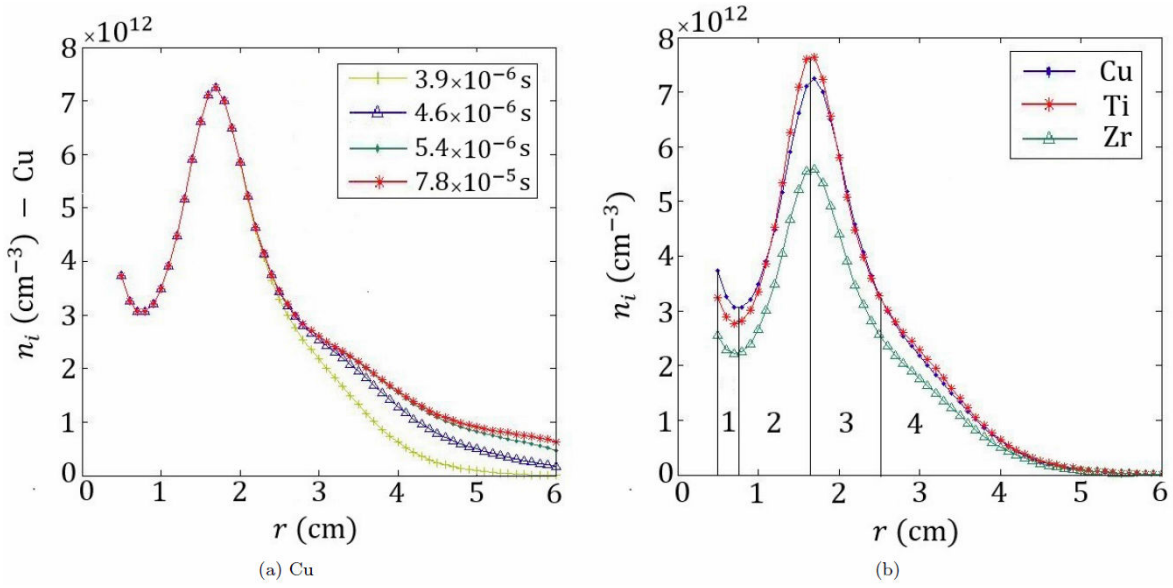

FIGURE 3. (a) Temporal evolution of ion density for Cu and (b) comparison of the profiles obtained for the selected materials at time $t = 3.9 \times 10^{-6}$ s.

the quasineutral condition in Eq. 5 determines the electron density (n_e) as:

$$n_e = z_r n_i, \tag{5}$$

Finally, we included the energy transport equation, taking into account flows and temperature equilibrium between species, and it is defined as:

$$\frac{3}{2}\frac{\partial}{\partial t}\left(n_e T_e\right) + \frac{1}{r^2}\frac{\partial}{\partial r}\left(r^2 q_e\right) = \frac{1}{\sigma}e^2 z_r^2 n_i^2 v_i^2 - \left(T_e - T_n\right) n_i \nu_{eq} - \frac{3}{2} n_e v_e \frac{\partial T_e}{\partial r}, \tag{6}$$

where $q_e = -\kappa_e \nabla T_e = -\kappa_e (dT_e/dr)$ is the Fourier electron heat flux and κ_e is the electron thermal conductivity. Also, $\nu_{eq} = (3/2)\,\delta_{en} v_{\text{th}} \sigma_{en} N_n$, being v_{th} is the electron thermal velocity, is the energy equipartition frequency between electrons and neutrals, and $\delta_{en} \sim 10^{-5}$ [24] is a parameter that represents the electron-neutral energy transference produced in a collision.

3. Results and Analysis

The results of the model are presented for a cathodic system operating in Ar gas environment at a discharge pressure of 1.7 mbar. The selected cathode materials for simulations are Cu, Ti and Zr, considering that these materials have been widely used for this type of processes. The initial values and constants used for the materials are presented in Table I. These values were published by Anders [25], and Gidalevich [23] for an arc discharge with similar characteristics of this model. Also, we have used experimental values obtained by Grondona *et al.* [10] using a discharge current $I = 100$ A, and discharge radius $a = 0.5$ cm, providing an ion current $I_r = 10$ A [26]. The model proposed by Kelly *et al.* [8] using the same set of parameters for the numerical solution of this model, showed that the ion current losses were almost total, giving as a result $v_e\,(a) = v_i\,(a)$.

An explicit finite differences numerical method was implemented to solve the set of equations presented in the model [27]. According to the initial velocities presented in Table I, and radial step selected $(r = 0.1$ cm), a time step $t = 7.81 \times 10^{-8}$ s was obtained. The first objective of the simulations is to find the presence of a steady state in the solution. In Fig. 3a, the profile of the ion density n_i is presented as a function of radius for different times for the case of Cu. The initial density at $a = 0.5$ cm was obtained using values presented in Table I, and equation for current density, $j = e n_i v_i z_r$. It can be seen, from the profile in Fig. 3a that, for $t = 7.8 \times 10^{-5}$ s, a convergence is achieved in the simulation since the solution does not differ because, it is seen from Fig. 3a that both curves are not exactly the same; it

means curves for $t = 5.4 \times 10^{-6}$ s and $t = 7.8 \times 10^{-5}$ s are quite similar, indicating the presence of a steady state. In the first interval $(0.5 \leq r < 0.7$ cm), our results can be compared with profiles of the same quantities from a steady model used in Ref. [7] and Ref. [28] obtaining a similar behavior.

In Fig. 3b, four intervals to study the behavior of ion density are included as follows:

- *Interval 1* $(0.5 \leq r < 0.7$ cm): It is observed, a decrease in n_i and a minimum at approximately $r = 0.7$ cm. This behavior is an indication of a spatial charge which is not in kinetic equilibrium (Knudsen layer) [29], since in this interval, the density is composed by two flows.The first flow is composed by particles that are evaporated from the electrode. The second one consists of atoms and ions, which flow from the plasma to the surface of the cathode. The difference in these flows is the variation in the kinetic energy E_i (Fig. 4). Thus, from $r = 0.7$ cm, an increase in the flow of ions to the cathode surface is observed.

- *Interval 2* $(0.7 \leq r < 1.6$ cm): In the included region of this segment, it was observed that as r move from a lower position to a higher one, n_i increases. This increase is due to pressure gradients accelerate the ions and enclose them in dynamic processes of the gas, such as ion−ion or ion−electron collisions regarded in Eqs. 1, 2, and 3. The atoms are ionized by the electrons that are emitted by the cathode, as well as by the plasma electrons with temperature T_e (Fig. 5). This process increases the ion density reaching a maximum value at a distance of 1.6 cm with respect to the cathode.

- *Interval 3* $(1.6 \leq r < 2.5$ cm): In this segment the ion density starts to decrease because of the recombination processes and the release of the electron energy. Initially, electrons have a much higher average velocity than ions, and therefore, they tend to flow out of the region of production much faster than ions [25], attenuating their temperature up to a length $r \approx 3$ cm, higher than the attenuation length of the kinetic energy for ions $r \approx 1.4$ cm (Fig. 4 and 5).

- *Interval 4* $(2.5 \leq r < 6$ cm): Finally, for this interval, the simulated densities of the three materials converge to zero, which is in agreement with experimental results obtained by Miyano *et al.* [30] where it is indicated that there is a slight dependence on the type of material of the cathode on the bulk of the plasma.

Concerning to the first interval, Grondona *et al.* [10] used a pulsed low−pressure arc operated with Ar gas filled at $p = 2$ mbar and $p = 10$ mbar using a Cu cathode. They obtained, from electrostatic probe measurements, some values of floating potentials, and ion flux in the outer-region of a pulsed low-pressure arc. The determination of n_i was carried out according to Lam's collisionless theory, having as a result, in this interval, a decrease of ion density, which is in agreement with our results. On the other hand, starting from the second and subsequent intervals, the results of ion density and kinetic energy behavior were confirmed experimentally by Zhu *et al.* [21]. They used a DC cathodic arc operated at the arc current of 50 A, with Mg cathode, and O_2 gas at pressures in the range of $0.7 \sim 3.0$ Pa. They found that the densities of Mg ions are strongly affected by the charge−exchange reaction, and deposition pressure. Also, they calculated the velocities of ions according to $v_i = v_i^0 + (2u_i^0/1 + e^{\alpha r})$, where v_i^0 is the velocity of the ion at $r = 0$, and α is a factor which depends of pressure. In the second interval, they attributed the increase of ion density to the exponential decay

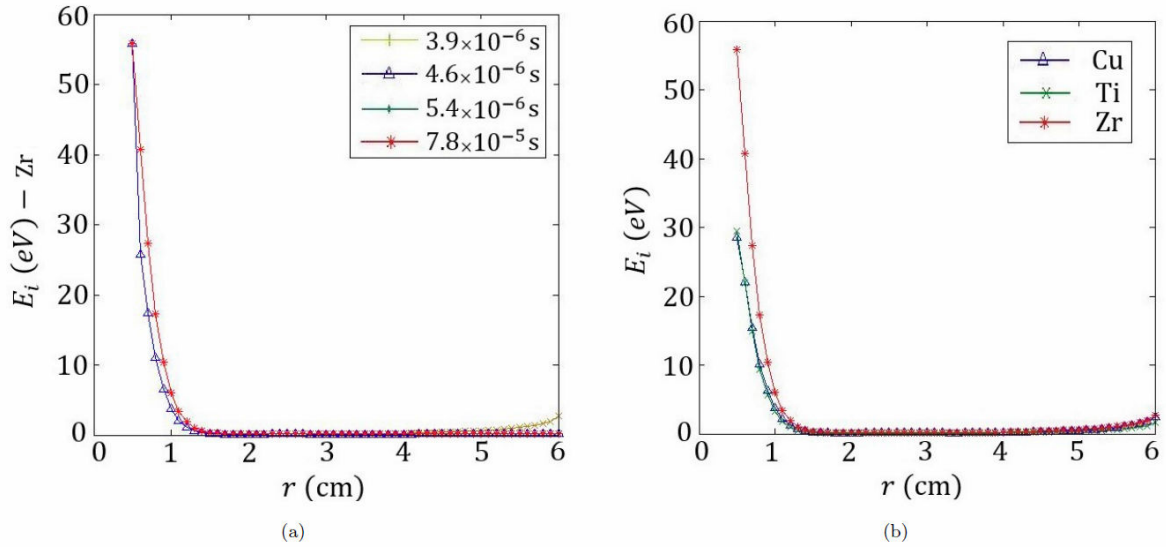

FIGURE 4. (a) Temporal evolution of the ion kinetic energy for Zr and (b) comparison of the profiles obtained for the selected materials at a time $t = 7.8 \times 10^{-5}$ s.

of velocity with r. Finally, in the third and fourth intervals, the velocity of ions decreases with the further increase of r (Fig. 4b). Moreover, the charge−exchange reaction is the dominant factor, and in consequence, the density of ions decreases as the radius increases.

The Fig. 4a shows the variation of the kinetic energy as a function of the radius at different times for Zr. A deceleration of the ions in the interval $(0.5 \leq r < 1.5$ cm) is observed. This behavior is due to the shock front that occurs between the metallic plasma and the neutral gas, abruptly reducing the energy of the ions by elastic collisions, until an uniform mixture of these volumes is reached.

On the other hand, Fig. 4b shows the variation of the kinetic energy as a function of the radius for the different materials at a time $t = 7.8 \times 10^{-5}$ s. From this figure, it is observed a considerable difference in the energy valued of the three simulated materials at $(r = a)$. This is due to the cohesive energy of each material of the cathode, which is the average binding energy of the atom in the solid. Zhu *et al.* [21] observed experimentally this phenomenon at positions near to the cathode surface. They found a reduction of the ion velocity which gives rise to a decrease in kinetic energy. These experimental results confirm our profiles for n_i, and E_i obtained in Fig. 3b and Fig. 4a with Zhu *et al.* observations. They also concluded that, the reduction of velocity of ions along the radius and the charge-exchange reaction can increase the density of ions, which is in agreement with our simulations.

Figure 5a shows the evolution of the electron temperature as a function of the radius at different times, for Cu. It is observed that the electrons have yielded their energy for a radius less than 3 cm. The energy released (heat) by these particles corresponds to the diffusion observed near the electrodes, affecting the thermal or random velocity. On the other hand, the time influence is observed, since in solving the system of equations simultaneously, in each iteration, the calculation of the electron is updated until finding the non−uniform convergence for a time $t = 7.8 \times 10^{-5}$ s.

Figure 5b shows the profile of the electronic temperature T_e, depending on the radius for the different materials at $t = 7.8 \times 10^{-5}$ s. There is no appreciable influence of the cathode material on the tendency of this variable, since the magnitude of the initial conditions of this parameter does not present a significant variation, since this value is related to the Joule heating. Consequently, it is also related to the current density, which is the same in all simulations (the energy gained by the electrons in the discharge comes from the Joule heating). Experimentally Grondona *et al.* [10] obtained, in the aforementioned experiment, at a pressure of $p = 2$ mbar, and $r = 1.75$ cm, an electron temperature of $T_e = 1.5 \pm 0.7$ eV. Likewise, García *et al.* [16] used a similar discharge device of Grondona *et al.* They generated the arc discharge in an atmosphere of N_2 at $p = 1.7$ mbar of pressure using three different cathode materials (Ti, Zr, and Al). Their studies gave as a result, values of electron temperature $T_e = 0.88$ eV for Zr, $T_e = 1.16$ eV for Ti, and finally $T_e = 1.22$ eV for Al. Additionally, both experiments confirm the decreasing tendency of the electron temperature. Comparing both results, we can conclude that the corresponding value, and the behavior obtained from the profile of our model simulations are in agreement with those experiments.

In Fig. 6a, the potential of the plasma ϕ, as a function of radius for various times is presented. The trend of this variable is similar to that of n_i (Fig. 4). When a large peak of charge concentration is formed around $r = 1.7$ cm, a maximum value of ϕ is produced around this value of r (Hump Theory: at the cathode contour, a region is produced where the potential is larger than that of the anode−cathode) [31].

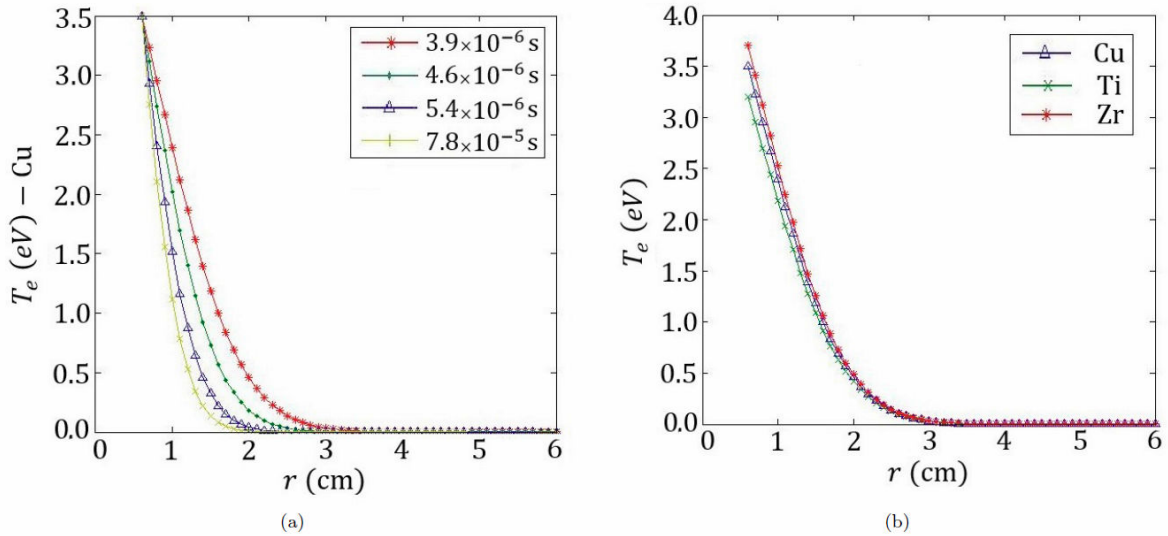

FIGURE 5. (a) Temporal evolution of the electron temperature for Cu and (b) comparison of the profiles obtained for the selected materials at a time $t = 7.8 \times 10^{-5}$ s.

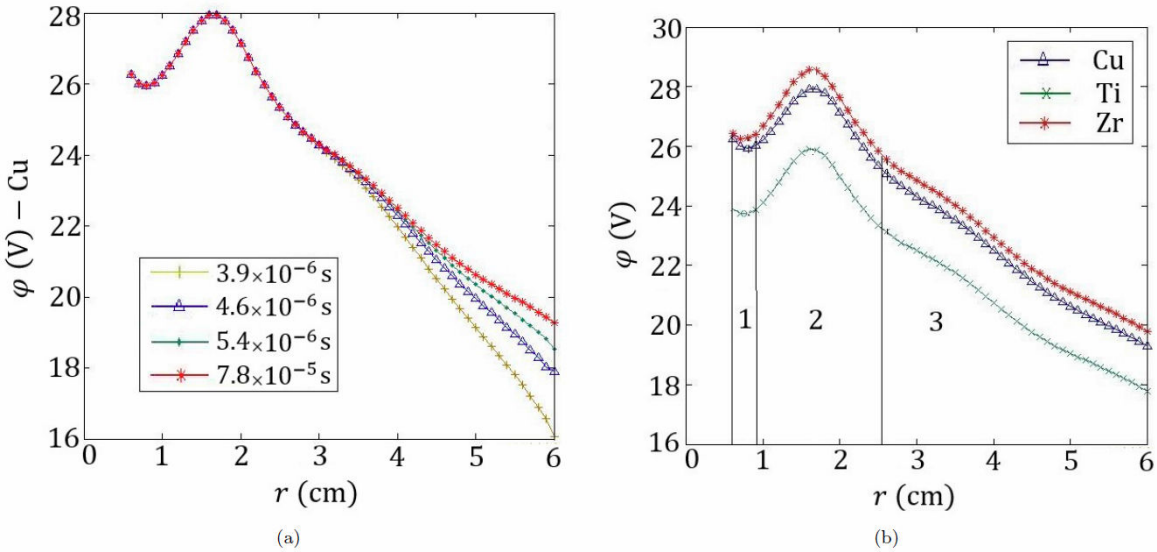

FIGURE 6. (a) Temporal evolution of the plasma potential for Cu and (b) comparison of the profiles obtained for the selected materials at $t = 3.9 \times 10^{-6}$ s.

In Fig. 6b three intervals are proposed to describe the behavior of ϕ as follows:

- *Interval 1* $(0.5 \leq r < 0.9\,\text{cm})$: It is observed a slight decrease; this is due to the evaporation of electrons and ions produced by the bombardment of the adjacent plasma. This leads to a non−stationary critical layer in the formation of the Hump potential, because it is not associated with the production of ion front to the cathode.

- *Interval 2* $(0.9 \leq r < 2.5\,\text{cm})$: In this segment. As this dense metal plasma expands, the protuberance of the potential travels with the ion front, and is decomposed as the density of these particles decreases at the time that the distance from the cathode increases, according to the considerations presented in Fig. 4.

- *Interval 3* $(2.5 \leq r < 6.0\,\text{cm})$: Finally, for this interval, the ion−electron drag and the electron−neutral moment transfer are much smaller than the electron pressure, and the electrostatic force, which provides the enough force to the ions for overcoming the shock front of the background gas, allowing them to reach the chamber walls.

In a partially ionized plasma, several important elastic and inelastic processes can simultaneously take place and they are responsible for redistributing the density, momentum and energy of the particles [32]. The collisions considered in Eq. (1), with the term $-m_i v_i^2 N_n \left[(m_n/m_i + m_n)\right] \sigma_{in}$, imply a moment exchange driven by the extreme pressure gradient, while the dissociative recombination processes included in Eq. (1), with the term $\left(-\left(\sigma_{\text{loss}} r^2 n_i v_i N_n\right)/Z_r\right)$, depend on v_i; therefore, there is a decreasing on the ions density, when they have yielded their energy (Fig. 4).

Concerning to cathode material dependency on the plasma variables. An experimental result is consistent with our simulations. In this study, Miyano *et al.* [12] using different cathode materials, and ambient gases, found that the cathode material does not affect directly the arc voltage behavior. They attributed this behavior due to the diameters of Ti, Cu and Zr atoms are similar (0.28, 0.27 and 0.31 nm, respectively), so that the collision cross-section between these metal ions and the gas molecules is not varied. Therefore, the ion deficiency forms at a similar pressure, and thus the flux emitted from the cathode changes at a similar pressure.

4. Conclusions

In this work, using numerical simulations, we have studied the plasma state generated by the interaction of a cathodic arc discharge and neutral particles. Taking into account the model developed by Kelly *et al.* [12]. We solved the system of equations to study the behavior of typical plasma quantities as a function of time, and distance from the cathodic region. Furthermore, we considered different cathode materials that are commonly employed in cathodic arc deposition. A decrease in the first stages of the evolution of the ion density was observed due to formation of Knudsen layer, which is represented by differences in kinetic energy between neutrals and ions; an increasing in later stages is due to pressure gradients accelerate the ions and enclose them in dynamic processes of the gas; at final stages, the ion density exhibited a decreasing trend following approximately Boltzmann relationship. The kinetic energy presented a deceleration. This behavior is due to the shock front that occurs between the plasma and the neutral gas, reducing the energy of the ions by elastic collisions, until a volume equilibrium is obtained. Regarding to the electron temperature, it was found that en-

ergy transference between electrons and ions is very low and is released as heat by these particles, which corresponds to the diffusion that they present near to the electrodes, affecting the thermal velocity. Moreover, the electric potential follows the same behavior of ion density, as expected. When a large concentration of particles is formed, a maximum value of potential is located in this zone; subsequently, the decreasing is controlled by electron pressure gradient because of the friction force between electrons and ions. Nonetheless, it is a fact that there is a small dependence on the cathode material. This is considered to be due to not only the size of the ions, but also their average charge, energy, and density. In spite of this result, it is suggested further investigations for qualitative and precise understanding. It is important to highlight the importance of these studies, due to the possibilities to guide experimental studies, where the objective is to obtain data about the structure of the cathodic arc discharge. Finally, the behavior of the electron temperature, ion density, and ion kinetic energy are in agreement with arc discharge experiments performed by different authors, giving rise to the reliability of the employed model.

Acknowledgments

We gratefully acknowledge the support of COLCIENCIAS via the Jóvenes Investigadores e Innovadores 2016 program, under the project No.077-2017 (206010014290) "Modelamiento teórico y desarrollo computacional de plasmas de laboratorio empleados en el procesamiento de materiales" and COLCIENCIAS Doctoral program Convocatoria 727 de 2015. We also give thanks to Universidad Nacional de Colombia and The Dirección de Investigación DIMA for its support.

1. D. S. Galeano-Osorio, S. Vargas, R. Ospina, E. Restrepo, and P. Arango *DYNA*, **81** (2014) 94,.
2. J. M. Albella, *Introducción a la ciencia de materiales: técnicas de preparación y caracterización*. CSIC Press: Madrid, (1993).
3. L. García, D. Escobar, J. De la Roche, P. Arango, and E. Restrepo *DYNA* **79** (2012) 90.
4. H. Kelly, F. Minotti, A. Márquez, and D. Grondona, *Meas. Sci. Technol.* **13** (2002) 623.
5. D. Grondona, H. Kelly, and F. Minotti, *J. Appl. Phys.* **99** (2006) 1.
6. R. L. Boxman and S. Goldsmith *IEEE Trans. Plasma Sci* **18** (1990) 231.
7. H. Kelly, A. Márquez, F. Minotti, and C. F. Fontán, *J. Phys. D: Appl. Phys.* **31** (1998) 1737.
8. H. Kelly, A. Márquez, and F. Minotti, *IEEE Trans. Plasma Sci*. **26** (1998) 1322.
9. J. L. Meunier and M. G. Drouet, *IEEE Trans. Plasma Sci.* **15** (1987) 515.
10. D. Grondona, H. Kelly, A. Márquez, and F. Minotti, *J. Phys. D: Appl. Phys*. **31** (1998) 3358 .
11. M. M. Bilek, P. J. Martin, and D. R. McKenzie, *J. Appl. Phys.* **83** (1998) 2965.
12. H. Kelly, A. Lepone, and F. Minotti, *J. Appl. Phys*. **87** (2000) 8316.
13. H. Kelly, A. Lepone, and A. Márquez *J. Appl. Phys.* **89** (2001) 1567.
14. D. Grondona, H. Kelly, A. Márquez, F. Minotti, and J. Zebrowski *IEEE Trans. Plasma Sci*. **28** (2000) 1280.
15. A. Lepone and H. Kelly, *J. Phys. D: Appl. Phys.* **34** (2001) 3043.
16. L. García, A. Pulzara, A. Devia, and E. Restrepo, *J. Vac. Sci. Technol A* **23** (2005) 551.
17. L. A. García, E. Restrepo, H. Jiménez, H. A. Castillo, R. Ospina, V. Benavides, and A. Devia *Vacuum* **81** (2006) 411.
18. F. O. Minotti, H. Kelly, and A. Lepone, *Plasma Sources Sci. Technol.* **11** (2002) 294.
19. E. Gidalevich, S. Goldsmith, and R. L. Boxman *J. Appl. Phys*. **90** (2001) 4355.
20. H. Changji, H. Zhenhui, F. Weichun, and Z. Qi, *J. Phys. D: Appl. Phys* **42** (2009) 185303.
21. D. Zhu, C. Zheng, D. Chen, and Z. He, *Plasma Sci. Technol* **15** (2013) 1116.
22. B. Juttner *J. Phys. D: Appl. Phys.* **14** (1981) 1265.
23. E. Gidalevich *Plasma Sources Science and Technology* **10** (2001) 24.
24. P. R. Yuri, *Gas discharge physics*. Springer: Moscow, (1997).
25. A. Anders, *Cathodic Arcs: From Fractal Spots to Energetic Condensation*. Springer Series on Atomic, Optical, and Plasma Physics, Springer: New York, (2008).
26. C. W. Kimblin *J. Appl. Phys.* **45** (1974) 5235.
27. S. C. Chapra and R. P. Canale, *Numerical methods for engineers*. McGraw-Hill Higher Education: Boston, (2006).
28. S. Ramírez, D. Sabogal, D. F. Devia, and E. Restrepo, *DYNA* **85** (2018) 76.
29. I. Beilis *IEEE Trans. Plasma Sci.* **35** (2007) 966.
30. R. Miyano, T. Saito, K. Kimura, M. Ikeda, H. Takikawa, and T. Sakakibara, *Thin Solid Films* **390** (2001) 192.
31. H. C. Miller *J. Appl. Phys*. **52** (1981) 4523.
32. V. L. Paperny, A. Chernich, N. Astrakchantsev, and N. Lebedev, *J. Phys. D: Appl. Phys*. **42** (2009) 155201.